Use of Neutron Reflection and Spectroscopic Ellipsometry for the Study of the Interface between Miscible Polymer Films

Bryan B. Sauer* and David J. Walsh

Central Research and Development Department, Experimental Station, E. I. du Pont de Nemours and Company, Inc., Wilmington, Delaware 19898

Received December 10, 1990; Revised Manuscript Received June 5, 1991

ABSTRACT: Specular neutron reflection (NR) and spectroscopic ellipsometry (SE) were used to investigate the interface between thin films of the miscible pair poly(vinyl methyl ether) (PVME) and polystyrene (PS). Interdiffusion of PVME (T_g = −31 °C) into PS (T_g = 104 °C) was quite rapid at temperatures more than 25 °C below the glass transition of polystyrene. The rate of change of the interface penetration depth into PS at 76 °C was markedly non-Fickian with an observed linear dependence with time. Interface profiles and interface dimensions were determined before and after annealing by the two techniques. Before annealing the interfacial thickness varied between 5 and 22 nm depending on original film thicknesses, and after annealing at 76 °C the interface broadened to ~55 nm. The factors controlling the broadening of the interfaces are discussed. Some evidence of asymmetric interfacial profiles with a low volume fraction of the more mobile PVME penetrating into the PS phase was also obtained with both techniques. The linear dependence with time and interface profile could be interpreted in terms of a case II diffusion process, which is typically seen for solvent penetration into glassy polymers.

Introduction

Few scattering techniques have been applied to the study of buried interfaces in the planar geometry because of the weak signal produced and the high spatial resolution needed. One must bring the probe particle (photon, neutron, X-ray, etc.) to the interface, and adsorption or bulk scattering can be a significant problem as compared to the study of free surfaces. Specular neutron reflection (NR) has an interfacial resolution of a fraction of a nanometer due to the small-probe wavelength and the high contrast when studying buried polymer interfaces between deuterated/hydrogenated species.[1] Polarized optical reflection methods such as frequency scanning ellipsometry (spectroscopic ellipsometry) (SE)[2] can also be used although the application to polymer interfaces has not been extensively explored.[3] One is limited to a certain extent by the small refractive index differences normally encountered with organic polymers, but deuteration is not necessary, making sample preparation more convenient. The main advantage is that with SE it is possible to probe macroscopic length scales (thousands of nanometers) with a resolution of the interfacial thicknesses generally in the range of 1–5 nm for refractive index differences between polymers on the order of 0.1.

Another advantage of using these two similar reflection techniques is that one can use NR in cases where its high resolution is needed and SE where large length scales are involved. On the other hand, because of the indirect nature of the interfacial profile determination, both techniques are lacking to a certain extent for the broad interfaces studied here. NR reflection suffers from the fact that it loses sensitivity in terms of quantifying dimensions of interfaces broader than a few hundred angstroms.[4] The fact that an interface may be asymmetric is even more detrimental because NR is mainly sensitive to the maximum density gradient in the interface profile although it is known that some information on the shape can be obtained if the interface is not too broad. SE suffers from lower resolution but has many advantages including precise layer thickness determination for thicknesses from a few nanometers to greater than several microns. One other difference is that the SE spectra are not dominated by the maximum gradient in the interface profile, so some features of the asymmetric profile are more obvious.

NR has been used to study very narrow interfaces such as the interface between the immiscible polymers, polystyrene/poly(methyl methacrylate) (PMMA).[5,6] X-ray reflectivity also gives the extremely high resolution needed for the interface between immiscible polymers such as PS/brominated PS.[7,8]

Closer to the topic of this paper, the interfaces between miscible polymers such as deuterated PS/hydrogenated PS[7,9,10] and PMMA/chlorinated polyethylene[11] have also been studied by NR. These polymer pairs have very similar glass transitions so they must be annealed above T_g. In the later case, it was found that the interface broadened slightly after annealing above the glass transition temperature (T_g) for a few hours,[11] but the interdiffusion process was quite slow. This is due to the slow diffusion rates of the polymers at the annealing temperature as has been shown by Rutherford backscattering spectrometry (RBS).[12]

FRES has been used to study the interdiffusion between PS and poly(xylenyl ether) (PXE; T_g = 217 °C). Similar to the polymers studied here, these two polymers have a large difference in glass transitions, and the interdiffusion was studied in the range 7–40 °C below the glass transition of PXE.[13] Although the variation of the interface position into the glassy PXE phase was plotted versus $t^{1/2}$ in their paper,[13] the two or three points at each temperature are not enough to verify this Fickian dependence with time.[14] On the other hand, the Fickian dependence of the PXE dissolution in the PS melt in the same experiment was well verified by the direct profiling technique.[13] We will show in this paper that the penetration of PS by PVME is markedly non-Fickian. With regard to the Fickian dissolution of the high-T_g species into the low-T_g phase that was seen directly by Composto and Kramer,[13] our techniques are not sensitive to the nature of the dissolution of PS in the PVME phase because of the low volume fractions of polymer involved.

A number of polymer interfaces have been studied by direct profiling techniques including RBS,[12,15] forward recoil spectroscopy,[16–19] and a nuclear reaction analysis technique.[20] NR and SE suffer because the data cannot be easily inverted in order to determine a unique interfacial profile. The direct techniques give the shape of the

0024-9297/91/2224-5948$02.50/0

interface unambiguously but with less resolution. A recent review of some of these results has appeared.[21] Dynamic secondary ion mass spectrometry (DSIMS) is also very useful in determining concentration profiles directly.[22,23]

One of the most extensively studied cases is interdiffusion between polymer A and polymer B, where A and B have similar glass transitions, such as in the case of isotopically labeled polymer pairs. A small difference in the diffusion coefficient gives rise to the phenomena of the "interface", as marked by tracer gold particles, moving toward the higher mobility phase. This occurs because the low-mobility polymer phase is swollen by the higher mobility polymer.[14] Because the polymers are annealed above their glass transitions, the diffusion is always apparently Fickian, and analyzing the broadening of the interface results in diffusion coefficients for the polymers. In the normal Fickian case where the annealing temperature is above T_g for both of the diffusing species, the nature of interfacial evolution is dominated by the more mobile of the two polymers.[21,24] Also, in Fickian diffusion, the characteristic rheological relaxation times are far-removed from characteristic diffusion times and there is no coupling between mechanical transitions and diffusion. In contrast, it is well-known that case II diffusion of solvent swelling and penetration into a glassy polymer well below T_g is strongly influenced by a coupling with mechanical relaxations in the glass.[25]

For the system of interest here, there is a large difference in mobility between PVME and PS. A temperature of ~80 °C is found to be convenient to study interdiffusion; at temperatures a few degrees higher the process is too fast to monitor quantitatively in thin (<1 μm) films, and at temperatures tens of degrees lower it is quite slow or negligible. Future experiments will address both of these regimes more thoroughly. This temperature of ~80 °C is above the glass transition T_g (-31 °C) for PVME and below the PS T_g (104 °C); thus, PVME is a fluid and is quite mobile, while PS is glassy and has essentially no center of mass mobility in the bulk. The disparity in mobilities leads to very asymmetric interdiffusion of the high-mobility species penetrating into the low-mobility one. The fact that one observes any penetration into PS at all 24 °C below the glass transition indicates that diffusive transport is not the only important variable. It will be shown that the interfacial position varies linearly with time, which is strong evidence that we are not observing a simple Fickian process, but one similar to case II diffusion typically observed for a solvent penetrating into glassy polymers.[25] Thus, mechanical relaxations in the glassy PS solid and the nature of the relaxation spectra as is related to the proximity to T_g are also very important, as has been proposed for the case of solvent permeation into glassy polymeric solids.[25] The asymmetric penetrant front,[25,26] consisting of a low volume fraction of PVME diffusing into the PS phase, is another indication that case II diffusion is occurring in this system.

Principles of Reflection

The basic equations governing the reflection of polarized light were derived by Drude.[27] The ratio of the reflection coefficients of the in-plane (R_p) and out-of-plane (R_s) polarized light is related to the two measured ellipsometric angles, the amplitude attenuation Ψ, and the phase difference Δ between the s and p waves:

$$R_p/R_s = \tan \Psi \exp(i\Delta) \quad (1)$$

For a single layer on a substrate the reflection coefficients for p or s polarization are

$$R = [r_{01} + r_{12} \exp(-i\beta)]/[1 + r_{01}r_{12} \exp(-i\beta)] \quad (2)$$

where

$$\beta = 4\pi n_1 d_1 \cos(\phi_1)/\lambda \quad (3)$$

and the indices 0–2 indicate air, film, and substrate, respectively, n_1 is the refractive index of the film, d_1 is the film thickness, ϕ_1 is the incident angle (measured from the normal to the surface) in the film, and λ is the wavelength. The Fresnel coefficients ($r_{i,j}$) for p or s polarization are related to the refractive indices and incident angles in each media and are defined as

$$r_{i,j(p)} = (n_j \cos \phi_i - n_i \cos \phi_j)/(n_j \cos \phi_i + n_i \cos \phi_j) \quad (4A)$$

and

$$r_{i,j(s)} = (n_i \cos \phi_i - n_j \cos \phi_j)/(n_i \cos \phi_i + n_j \cos \phi_j) \quad (4B)$$

where the subscripts i and j are the substrate indices as defined above. All these equations are used together to define an algebraic relationship for the reflection coefficients in eq 1, which is then solved numerically to give the simulated profiles of Ψ and Δ. Iterative schemes can be used to build up reflection equations for multilayer systems.[28]

In neutron reflection only the absolute reflected neutron intensity is measured. All phase information is lost, yet very high resolution can be obtained because of the small wavelength, which is varied between ~0.2 and ~1.5 nm here. For the single-layer case, the intensity is given by the square of eq 2[29]

$$|R|^2 = \frac{(r_{01}^2 + r_{12}^2 + 2r_{01}r_{12} \cos \beta)}{(1 + r_{01}^2 r_{12}^2 + 2r_{01}r_{12} \cos \beta)} \quad (5)$$

where $|R|^2$ is the total reflected intensity (or reflectivity). Iterative schemes are also used to build up reflection equations for multilayer systems. The effective neutron refractive index is defined as[30]

$$n^2 = 1 - \lambda^2(b/V)/2\pi \quad (6)$$

where b is the scattering length and V the volume per scattering center, with the term b/V commonly referred to as the scattering length density.

To include an interfacial density gradient, a Gaussian density profile across the interface between the i and j layers can be assumed by modifying each Fresnel coefficient[31]

$$r_{i,j} = (n_j \cos \phi_i - n_i \cos \phi_j)/(n_j \cos \phi_i + n_i \cos \phi_j) \exp(-2q_i q_j \langle z^2 \rangle) \quad (7)$$

where

$$q_i = 2\pi \sin(\theta_i)/\lambda, \quad q_j = 2\pi \sin(\theta_j)/\lambda \quad (8)$$

are the momentum transfers in each respective media, $\langle z^2 \rangle$ is the mean-squared roughness, and θ is the grazing angle of incidence ($\theta = 90° - \phi$). With a given technique, one cannot generally distinguish roughness up to a certain length scale from interfacial broadening due to interdiffusion.

Experimental Section

The narrow molecular weight distribution hydrogenated PS and deuterated PS samples both had M_w = 104 000 with T_g = 104 °C. The PVME (repeat unit CH_2CHOCH_3) was obtained

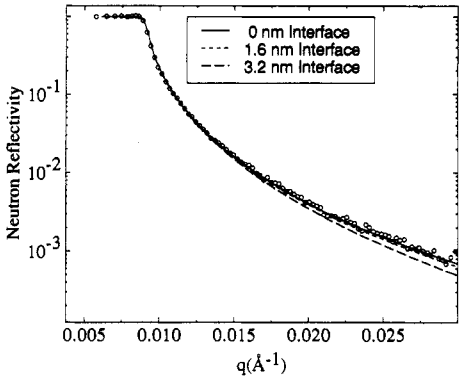

Figure 1. Neutron reflectivity versus neutron momentum (q) for a film of deuterated PS (~800 nm thick) on glass. The PS layer is effectively infinite in thickness to the neutrons so the reflectivity is governed by only two parameters: surface roughness at the air/polymer surface and the neutron scattering length density (b/V), which was determined to be 6.5 (±0.05) × 10^{-10} cm^{-2}.

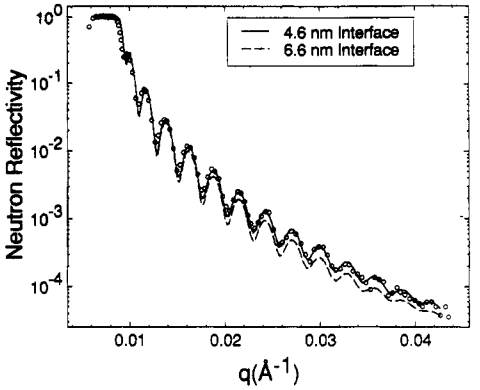

Figure 2. Neutron reflectivity vs q for as-spun films of PVME (350 nm)/deuterated PS (102 nm)/glass. The best fit is to a 4.6 ± 0.2 nm linear gradient interface, and a simulated profile for a 6.6-nm interface is shown for comparison. Parameters are compared with those determined by SE for the same sample in Table I.

from Polysciences and had a M_w of 99 000 with $M_w/M_n = 2$ and $T_g = -31$ °C. Preliminary experiments on a PVME sample, which was reprecipitated in order to remove the low molecular weight tail, indicate that this level of polydispersity does not change the general features observed here. Approximately 10% solutions of hPS and dPS in xylene were filtered with 0.45-μm PTFE filters and then spin-coated onto uncoated Pyrex mirrors (Melles Griot; 5-cm-diameter Pyrex borosilicate glass, smooth to λ/10). All PS films were annealed at 120 °C to remove solvent and relax residual polymer orientation. The PS layer thickness was determined by ellipsometry before spin coating the PVME layer to indicate the quality of the film and also to help in making the initial guesses for the film thicknesses in the multilayer experiments. The PVME films were spun from solutions of n-butyl alcohol, which is a nonsolvent for PS. PVME was spun directly onto the PS layer. Because PVME is known to absorb water, a special chamber was made so the ellipsometry experiments could be run under dry N_2. The ellipsometry results were not found to be affected by ambient humidity so all of the data presented were obtained under ambient conditions.

To rapidly bring the sample to elevated temperatures, a brass plate (~0.5 kg) was first heated to ~20 °C above the desired annealing temperature. The glass flat was then placed on the hot brass plate in the oven set to the desired temperature. The temperature was monitored by a microthermocouple taped to the top of the glass substrate. The sample could be heated from 25 to 80 °C in ~60 s in this manner. The glass flats were 10 mm thick, and it was sometimes difficult to control the temperature, resulting in an accuracy of approximately ±2 °C.

The spectroscopic ellipsometer and analysis software were supplied by Sopra (distributed by Aries, Concord, MA 01742). A typical spectra covering 80 wavelengths between 300 and 700 nm took about 15 min. The NR experiments were performed at Argonne National Laboratories by using the pulsed source and the POSY II spectrometer with a time-of-flight detector. Each spectrum was obtained by signal averaging for 1–4 h.

Results

Air/Polymer Surface Roughness Studied by NR. Figure 1 shows a plot of neutron reflectivity as a function of neutron momentum ($q = 2\pi \sin(\theta)/\lambda$) for a film of deuterated polystyrene on glass. The grazing angle of incidence (θ) is on the order of 0.8°. The 800-nm PS layer is effectively infinite in thickness to the neutrons, so the reflectivity is governed by only two parameters: surface roughness at the air/polymer surface and the neutron scattering length density (b/V). The advantage of having an infinitely thick film is that roughness on the glass side of the film and thickness variations do not influence the spectra, making the experiment a better test of roughness on the free polymer surface. The best fit using the linear gradient interface profile was close to zero, with an estimated precision of ±1 nm. A scattering length density for deuterated PS of 6.5 (±0.05) × 10^{-10} cm^{-2} was determined from the fit in agreement with published tables.[32] Profiles generated using various linear gradient interfacial thicknesses are shown in the figure to indicate the sensitivity. This allows one to define an upper limit of the air/polymer interfacial width in terms of the segmental density profile normal to the surface, since this is indistinguishable from roughness. Another convenient method of modeling interfaces is by using the error function (eq 7), which defines the interface in terms of a Gaussian segmental density profile normal to the interface. Some discussion of these different profiles has been made earlier.[6] From the error function fit the roughness parameter ($\langle z^2 \rangle^{1/2}$, which is equivalent to interfacial width) is obtained which defines the exponential decay length of the segmental density profile. Numerically, because of the way the error function parameter is defined, it has to be multiplied by ~2 to be consistent with the thickness determined by fitting to the linear gradient profile. This factor of ~2 was determined by matching the profiles generated by the two models for the ranges of momentum transfer (q) and interfacial thicknesses (~3–20 nm) for polymer/polymer interfaces studied in this paper. Thus, here and in all the discussion that follows, we will present the interfacial dimensions in terms of the equivalent of the linear gradient profile, i.e., the error function width $\langle z^2 \rangle^{1/2}$ times 2.

Table I
Comparison of Fitted Parameters for the As-Spun Bilayer: PVME (350 nm)/dPS (102 nm)

	ellipsometry		
	a	b	NR[c]
PVME thickness, nm	346	332	350[c]
interface thickness, nm	5.8 ± 3.0	30[b]	4.6 ± 0.2
dPS thickness, nm	102	92	101.7
χ^2	0.0097	0.0129	c

[a] Best fit to interface and layers. [b] Interface was fixed to an unreasonable value of 30 nm in order to compare statistics of the fit (see Figure 8). [c] NR data on the same sample. The PVME layer thickness was too large to measure, and χ^2 is not relevant here.

As-Spun PVME/PS Films, NR. The reflectivity profiles for an as-spun PVME/PS/glass bilayer sample are shown in Figure 2. Once again, NR is not sensitive to the PVME layer thicknesses (~346 nm; Table I) but is sensitive to the PS layer thickness (~100 nm) and the interfacial broadening. For interfacial thicknesses on the

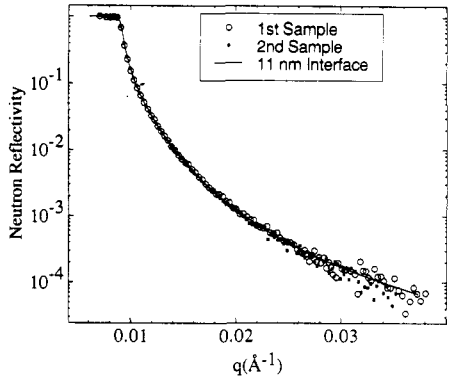

Figure 3. Reflected neutron intensity versus momentum transfer (q) for PVME (800 nm)/deuterated PS (800 nm)/glass. The reflectivity profiles for two different as-spun bilayer samples are plotted. The data indicate that the reproducibility of the experiment is quite good from sample to sample. The solid curve is the best fit, giving an "error function" thickness of 5.5 nm or a linear gradient thickness of 11 nm, and $b/V = 1.6\ (\pm 0.1) \times 10^{-10}$ cm^{-2} for the PVME phase. All interfacial thicknesses are reported in terms of the linear gradient profile in order to facilitate a direct comparison with the ellipsometric thicknesses.

order of 10 nm, a crude model such as the step-profile interface did not fit the NR data because one starts to see a hint of interference fringes. A simulated profile calculated using an error function parameter $\langle z^2 \rangle^{1/2}$ equal to 2.3 nm corresponding to a linear gradient profile width of 4.6 ± 0.2 nm is shown in Figure 2. The quality of the fits for these films using the two different profiles was the same within experimental error, and the origin of this factor of 2 difference was discussed in the previous section. The similarity in quality of fit arises because the reflectivity is governed mainly by the maximum density gradient, leading to a negligible effect of the tails of the error function profile for this q range. The SE (to be discussed later) and NR results on the same sample are collected in Table I. Ellipsometry gives the interface as 5.8 ± 3 nm, which is in reasonable agreement with the NR value of 4.6 ± 0.2 nm discussed above. This substantial interface for the as-spun sample is probably due to our preparation method of spin-coating the PVME directly onto PS even though n-butyl alcohol is a solvent for PVME but is a nonsolvent for PS. The as-spun interface thicknesses range from 3 to 25 nm for different samples, with the broader interfaces generally corresponding to thicker PVME films because of slower solvent evaporation. The scattering length density determined from the data for the PVME layer was $b/V = 1.6\ (\pm 0.1) \times 10^{-10}$ cm^{-2} for PVME in good agreement with the value calculated based on chemical composition. The value of b/V for deuterated PS was again $6.5\ (\pm 0.05) \times 10^{-10}$ cm^{-2}.

80 °C Annealing of PVME/PS Films, NR. All elevated temperature annealing experiments presented here are for thick (~800-nm PVME/800-nm deuterated PS) bilayer samples, similar to those studied by SE (data presented later). Spectra for two separate as-spun samples are given in Figure 3, indicating that the samples can be prepared reproducibly. Figures 4 and 5 illustrate the changes that are observed after annealing for 2 and 12 min at 80 °C, respectively. Symmetric profiles were fitted to the NR spectra as was discussed above, and the fits are indicated in the figures and the parameters are given in Table II. Profiles generated with a wide range of interfacial thicknesses are shown in Figure 4 to illustrate the theoretical effect on the reflectivity. The NR interfaces using the symmetric fit are on the order of 10 nm for the annealed samples and are apparently much narrower than the ~50-nm interfaces measured by ellipsometry (Table III). This apparent discrepancy can be explained in terms of an asymmetric interfacial profile that evolves during annealing, which is one signature of non-Fickian diffusion.[26,33] Upon closer examination of the symmetric fit to the 12-min annealed sample (inset, Figure 5), it is evident that there is a slight deviation from experiment in the vicinity just past the critical angle. It is found that, by assuming a low volume fraction tail of PVME extending into the PS layer, the reflectivity will be moderated in the critical region in this fashion. The asymmetric interfacial

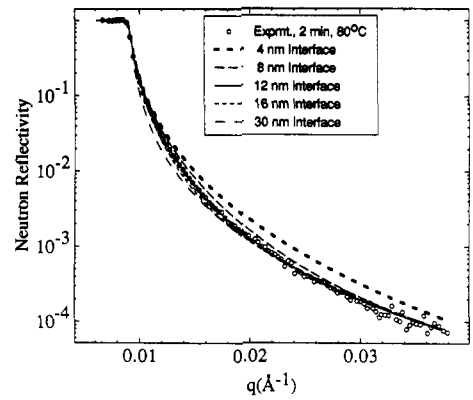

Figure 4. Reflectivity curve for the sample from Figure 3 annealed for 2 min at 80 °C plotted along with various simulated spectra for interfacial thicknesses from 4 to 30 nm using $b/V = 2.0\ (\pm 0.2) \times 10^{-10}$ cm^{-2} for the PVME phase. The best fit is 12 nm.

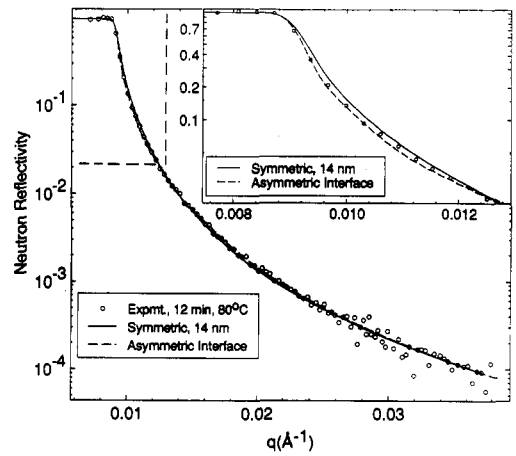

Figure 5. Reflectivity vs q for the sample from Figure 3 annealed at 80 °C for 12 min. The best fit using the 14-nm symmetric profile is shown as the solid curve, and the dashed line was generated by using the asymmetric profile shown in Figure 6. The value of b/V of the PVME phase also apparently increases to 2.7 (±0.2) × 10^{-10} cm^{-2}, indicating that the PVME phase contains 22% dPS. The asymmetric profile gives a better fit in the low-q region, as is indicated in the inset. The asymmetric profile is not a unique one but is consistent with the ellipsometry data (see text).

Table II
Annealing Effect on the Interfacial Thickness of PVME/PS[a] Neutron Reflection

	interfacial thickness,[b] nm	$(b/V)_{PVME}$,[c] $\times 10^{-10}$ cm^{-2}
as-spun	11 ± 1	1.6 ± 0.1
2 min at 80 °C	12 ± 2	2.0 ± 0.2
12 min at 80 °C	14 ± 2	2.6 ± 0.1

[a] Both films were ~800 nm thick. See ellipsometric results for precise thickness determinations. [b] The symmetric interfacial thicknesses are presented here for the annealed samples, keeping in mind that a better fit is obtained by using a broader asymmetric interfacial profile such as that in Figure 6. [c] The values of b/V are increasing because of the dissolution of PS into the PVME phase.

Table III
Variation of the Ellipsometric Layer and Interface Thickness as a Function of Annealing Time (min) and Temperature (°C)

	time	temp	thickness, nm PVME[a]	interface[b]	PS	χ^2
			1st Sample			
1.	as-spun		743 (100% PVME)	24 ± 10	814	0.0148
2.	8	57	739 (100% PVME)	29	812	0.0170
3.	8	67	740 (100% PVME)	31	811	0.0161
4.	5	76	734 (100% PVME)	48	795	0.0161
5.	15	76	773 (97% PVME)	54	756	0.0135
6.	25	76	818 (92% PVME)	62	699	0.0150
7.	35	76	848 (90% PVME)	45	675	0.0137
8.	45	76	885 (84% PVME)	54	638	0.0140
			2nd Sample			
1.	as-spun		750 (100% PVME)	20 ± 7	841	0.0142
2.	5	76	738 (100% PVME)	51 ± 8	824	0.0128

[a] Composition determined by ellipsometry from the refractive index of the PVME phase. [b] The interface used was a symmetric linear gradient profile.

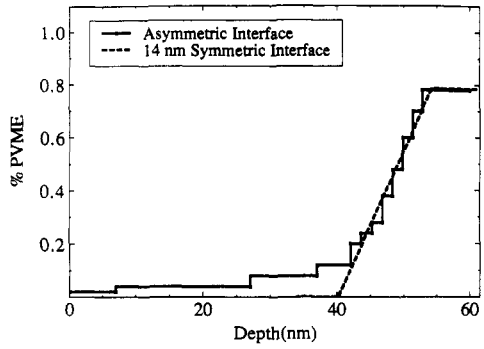

Figure 6. Interfacial profiles used to fit NR data in Figure 5. The asymmetric profile gives an improved fit to both neutron and ellipsometry data for annealed samples.

profile shown in Figure 6 was used to generate the reflectivity spectra indicated in the inset of Figure 5, leading to better agreement with experiment. The linear gradient profile used in the "symmetric" fit in Figure 5 is also shown for comparison in Figure 6. Note that under these conditions of 12 min of annealing at 80 °C that there is 22% deuterated PS dissolved in the PVME phase. This concentration was calculated from the b/V value of 2.7 (±0.1) × 10^{-10} cm^{-2} for the PVME phase, which is well defined by the reflectivity spectra at high q. The dissolution of PS into PVME is expected[13] and will be discussed in more detail later.

Spectroscopic Ellipsometry Study of Single Layers. To model the SE data, a refractive index (n) "basis file" as a function of λ must be generated for polymers and substrate. Values of $n(\lambda)$ for the polymer are readily determined via ellipsometry, using an optical quality polymer film of known thickness and back calculating $n(\lambda)$ from Ψ and Δ. From data for a single layer of PS on Pyrex (Figure 7), the refractive index of PS can be determined. The values $n(\lambda)$ obtained agree well with the literature values for $\lambda \geq 300$ nm.[34] The refractive index of PS ranges from $n = 1.695$ at $\lambda = 300$ nm to $n = 1.591$ at $\lambda = 600$ nm. Refractive indices were also determined from the measured Ψ and Δ for PVME (spin-coated on silicon) ranging from $n = 1.504$ at $\lambda = 300$ nm to $n = 1.465$ at $\lambda = 600$ nm.

Using the refractive index basis file for PS, a one-parameter nonlinear regression of tan Ψ and cos Δ as a function of λ results in a thickness of 821.3 ± 0.2 nm for the data in Figure 7 (solid line). A simulated profile is also shown for a thickness of 831.3 nm to give an idea of

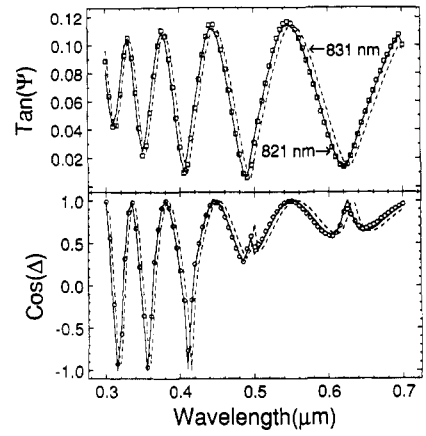

Figure 7. Ellipsometric angles tan Ψ and cos Δ plotted vs wavelength for a 821.3 ● 0.2 nm PS film on glass using an incident angle measured normal to the surface of $\phi = 60°$. Simulated profiles are also shown for a thickness of 831.3 nm for comparison.

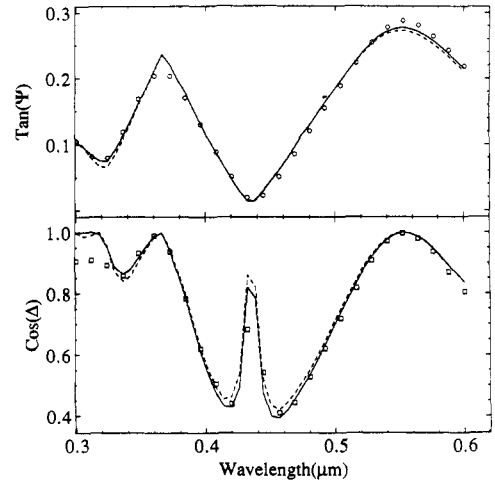

Figure 8. Ellipsometry data for as-spun films of PVME (346 nm)/deuterated PS (102 nm)/glass. The solid curve is the best fit, resulting in a 5.8 ± 3.0 nm linear gradient interface. The dashed curve is a simulated profile for the sake of comparison, fixing the interface at an unreasonable value of 30 nm. NR data were collected on the same sample, giving an interface thickness of 4.6 ± 0.2 nm.

the sensitivity to thickness. Including roughness at the air/polymer or glass/polymer interfaces did not give any improvement in the quality of the fit. The free polymer surface is apparently smooth to ~1.0 ± 1 nm, consistent with the NR experiments.

SE Studies of As-Spun Bilayers. Data for the same as-spun bilayer comprised of 346-nm PVME on 102-nm deuterated PS that was discussed earlier in the context of NR are shown in Figure 8. With a symmetric profile, the best fit was obtained with the thicknesses listed in the first column of Table I. Regression was performed on tan Ψ and cos Δ simultaneously to minimize the sum of the square of the deviations using three parameters (two film thicknesses and one interface layer). The best fit gives an interfacial thickness of 5.8 ± 3 nm, consistent with the NR value of 4.6 ± 0.2 nm for the same sample. For the sake of visual comparison on this plot, the interface width was fixed at an unreasonably large value of 30 nm and then the best fit was obtained by varying the layer thicknesses, resulting in the dashed curve (Figure 8). Although the difference is small, it is evident that the fit is better for the 5.8-nm interface, and statistically the improvement (Table I) in the fit is quite significant and is ~30%.

SE Studies of Annealed Bilayers. For films of PVME (T_g = −31 °C) on PS (T_g = 104 °C), a temperature of 76

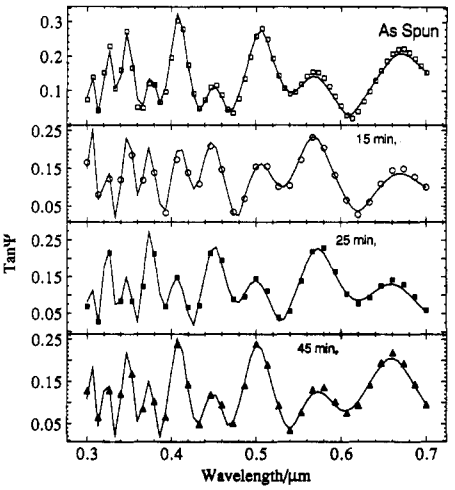

Figure 9. Tan Ψ vs wavelength at $\phi = 60°$ for thick layers of PVME/PS/glass for different annealing times at 76 °C. Solid curves are profiles determined by using nonlinear regression, giving the parameters listed in Table III.

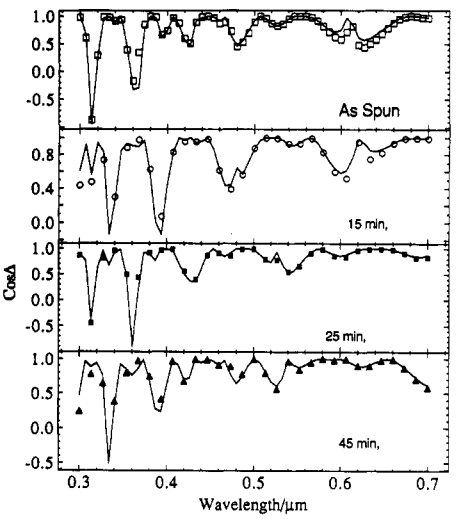

Figure 10. cos Δ vs wavelength at $\phi = 60°$ for PVME/PS/glass for different annealing times at 76 °C. Solid curves are profiles determined by using nonlinear regression, giving the parameters listed in Table III.

°C was found to be convenient to perform sequential annealing experiments. It was found later that the rate of PVME penetration into PS actually varies by more than 1 order of magnitude in the region 70–80 °C, so the 80 °C NR anneal experiments discussed above were performed at a temperature where interdiffusion occurred slightly faster. The general features of interdiffusion of PVME/PS do not seem to change over this range. The miscibility behavior of deuterated and hydrogenated PS in PVME has been discussed in a recent review.[36] The phase diagrams indicate that the minimum in the coexistence curves is about ~35 °C lower for hPS (infinite MW value, 95 °C) as compared to dPS (infinite MW value, 130 °C).[36] Thus, the driving force for interdiffusion should be higher for dPS than hPS, and some of these effects will be investigated in the future.

The films used here were relatively thick in order to monitor interdiffusion over macroscopic distances. Approximately 800-nm-thick films of PVME on ~800-nm PS were studied, and the as-spun interface thicknesses are on the order of 20 nm (Table III). This broader interface is most likely related to slight surface swelling of PS during spin-coating while the *n*-butyl alcohol was evaporating from the thicker PVME layer.

The SE spectra obtained for the bilayer system in Figures 9 and 10 exhibit complicated interference profiles because of the relatively large layer thickness relative to λ. As the sample is successively annealed at 76 °C, the spectra shown change in a rather subtle manner. The spectra were obtained after annealing the sample at 76 °C and then recording the SE spectra within 10 min. Regression on tan Ψ and cos Δ assuming a symmetric linear gradient interface profile gives the parameters listed in Table III. It is evident that the interface broadens to a constant value of 54 ± 8 nm, as compared to the original ~22-nm interfacial thicknesses for the as-spun samples. At room temperature no changes were observed over a period of months. At 57 and 67 °C it was difficult to see any significant change over a period of a few minutes (Table III). Above 90 °C interdiffusion was too rapid to be monitored sequentially even though this temperature is slightly below T_g of PS. It is determined that after 45 min at 76 °C the PS layer thickness decreases by almost 176 nm, and the PVME layer thickness increases by 142 nm. Because of the increase in interfacial thickness at the start, the overall thickness of the system remains constant.

The fit can be improved by adjusting the PVME layer composition to account for the PS dissolution. It was found that the refractive index of the PVME layer increased, as is shown in Table III in terms of a lowering of the volume fraction of PVME. The values agree qualitatively with those expected based on the change in layer thicknesses. The precision of this determination is roughly ±2%. The refractive index of the unswollen PS layer is found to remain constant as expected.

Discussion

Asymmetric Interface Determined by SE. The results of fit to the SE data using a symmetric interface (54 ± 8 nm) after annealing (Table III) are distinctly different from those determined by the symmetric fit to the NR data, which resulted in an apparent 14-nm interface. Since the symmetric profile is not really the correct profile, this apparent discrepancy occurs because NR is very sensitive to the maximum density gradient of the interface while SE gives a more equal weighting to all features of the interface. In fact, if one generates a theoretical SE spectrum using the asymmetric interface profile shown in Figure 6 and then takes this simulated data set and performs another fit assuming a symmetric profile, the best fit results in a symmetric interface width of 44 ± 5 nm, while the symmetric NR fit would give 14 nm. It is evident that this difference in the sensitivity of SE and NR explains qualitatively the discrepancy when fitting an asymmetric interface profile with symmetric interfaces.

We now proceed to the modeling of the SE data using the same asymmetric profile, shown in Figure 6, that was used previously to fit the NR data. It should be kept in mind that the improvement in fitting of the SE data with the asymmetric interface is small and some of the profiles used are not completely unique, but it will be shown that the results are qualitatively consistent with those obtained by NR. Small perturbations (<15%) in the dimensions of the profile shown in Figure 6 were allowed in the regression procedure for the SE data. The resulting χ^2 values are given in Table IV and are compared with those obtained earlier by using a symmetric profile to fit the data. It is evident that χ^2 is systematically reduced (~10% improvement) by using the asymmetric profile to fit the data. Thus, the SE data are consistent with those obtained

Table IV
Comparison of the Modeling with Symmetric and Asymmetric Interface Profiles. Statistics for Goodness of Fit of Ellipsometry Results[a]

time, min	temp, °C	PVME,[a] %	symmetric interface,[b] nm	χ^2 sym interface	χ^2 asym interface[c]
15	76	97	54	0.0135	0.0121
25	76	92	62	0.0150	0.0148
35	76	90	45	0.0137	0.0125
45	76	84	54	0.0140	0.0134

[a] Results from Table III. [b] Interfacial widths in terms of linear gradient profiles are given here (see Table III). [c] Asymmetric profiles roughly equivalent to that given in Figure 6 are used here. Statistically, there is a small improvement in the goodness of fit using the asymmetric profile (see text).

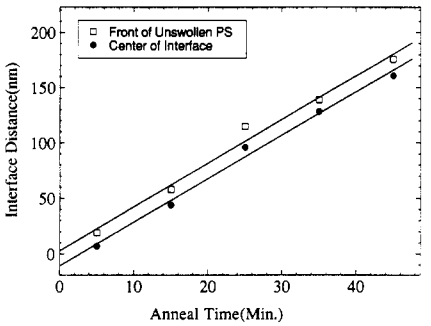

Figure 11. Non-Fickian variation of penetration depth (interface distance) into PS as a function of annealing time at 76 °C. The linear dependence indicates case II diffusion. The open squares were determined by the change of the PS layer thickness defined as the boundary between swollen and unswollen material, and the filled circles are points relative to the center of the interface. Data are from Table III.

by NR, and future experiments using a variety of techniques will allow a more quantitative determination of the profile. The asymmetry on the PVME side of the interface in terms of PS dissolution and diffusion into PVME cannot be quantitatively determined because of the low volume fractions involved. It is possible to determine the PS volume fraction in PVME by determining the layer refractive indices as was discussed above.

Evidence for Case II Diffusion. Plotting the data in Table III in terms of the change in PS layer thickness vs t gives the open squares in Figure 11. The results indicate a marked deviation from Fickian (or $t^{1/2}$) dependence. The same trend is observed, when the penetration depth into PS calculated relative to the center of the interface is plotted (filled circles). The linear dependence could be interpreted as case II diffusion similar to that observed for solvent penetration of glassy polymers at temperatures well below T_g of the glassy polymer. The asymmetric profile of PVME extending into PS (Figure 6) is also consistent with those determined for case II diffusion of solvent.[26,33] In these studies of solvent case II diffusion, detailed profiles of the Fickian precursor of the solvent ahead of the case II front in the glassy polymer were also determined. We do not have sufficient resolution to observe the Fickian precursor at this time. It is known that a complete theoretical description is not available for us to model the influence of mechanical relaxations on penetrant diffusion in the glassy plasticized solid, as related to case II diffusion.[33] Improved models have been recently developed and applied successfully to describe solvent/polymer case II diffusion,[35] and this theory will be used to model PVME/PS in the future.

Dissolution of PS into the PVME Phase during Annealing. Because of the high rate of PS dissolution on the PVME side of the interface at 76 °C, the interface for 100K PS/100K PVME never broadens to more than ~55 nm. The interface thickness is kinetically controlled by a fine balance between the rate of penetration of PVME into PS (interpreted as a case II penetration rate), competing with the rate of PS dissolution into the PVME phase. For very fast dissolution of swollen PS relative to the rate of penetration, the interface stays relatively sharp. For very slow PS dissolution relative to the rate of PVME penetration into the PS phase, very broad asymmetric interfaces would be expected. This later case should occur with high molecular weight PS or at high temperatures because both of these slow down the relative PS dissolution rate as compared to the PVME penetration rate. For example, increasing the MW of PS by 10-fold to 1000K allows one to generate very broad asymmetric interfaces by annealing at 76 °C because of the slow dissolution rate of 1000K PS.

Table V
Room-Temperature Interfacial Narrowing as a Function of Time after Annealing at 78 °C for 2 min As Determined by Ellipsometry

	thickness, nm PVME	interface[a]	PS	χ^2
as-spun	412	21 ± 6	390	0.0077
10 min after anneal	430	55 ± 8	339	0.0123
5 days after anneal	440	31 ± 6	348	0.0086

[a] Interface chosen as symmetric linear gradient profile.

A related question is whether the dissolved PS completely disperses in the PVME phase during annealing. For the case of 10-min anneal steps at 76 °C where approximately 40 nm of the PS layer is dissolved away per anneal step (Table III), the dissolved PS must diffuse through the PVME matrix over a distance of ~800 nm. Complete dispersion at the annealing temperature during the short annealing and quenching times probably does not occur. However, within the accuracy of our determination it does disperse to a large degree since a refractive index increase of the PVME phase is readily detected due to dissolved PS. Because of the high mobility of PVME at 25 °C, dissolved PS also continues to disperse after quenching to room temperature. Quantitative measurements of this diffusion rate should be possible in the future. This tracer diffusion of the dissolved PS under very dilute conditions at room temperature is much more rapid than the interface sharpening discussed below. This is because, for the interface sharpening case, the PS volume fraction is quite high, reducing mobility.

Room-Temperature Diffusion and Interfacial Sharpening. We end this section with several observations and comments related to the occurance of diffusion at room temperature and how this influences the results obtained by the two techniques. Even though there is no penetration of PVME into the glassy unswollen PS phase at 25 °C, there is the possibility of diffusion in the PVME phase at low PS concentrations because of the low T_g (−31 °C) of PVME. One consequence of this is that, after high-temperature annealing, interfcial sharpening at 25 °C occurs as interfacial material with a high PVME volume fraction is free to diffuse while the material with a low volume fraction of PVME is below its effective T_g at 25 °C and is immobile. We do not see this sharpening for the as-spun samples, presumably because of the rather sharp interfaces (interface thickness is less than or approximately equal to the chain dimensions). An example of interfacial sharpening is given in Table V where 10 min after annealing at 78 °C for 2 min the interface width is 55 ± 8 nm, which

then narrows to an asymptotic value of 31 ± 6 nm after 5 days at 25 °C. This feature is important if one wishes to compare techniques because, while SE spectra were obtained immediately after annealing, the NR data acquisition was started about 2 h after annealing and the data (Figure 5) were collected over a ~3-h time period. These longer induction times before and during the measurement could lead to some changes in the interfacial dimensions during the NR data collection. However, we do not feel that they have influenced the conclusions made here with respect to the comparison of the techniques.

Conclusions

SE and NR were used to study the interface between the miscible pair PVME/PS as a function of temperature and time. As-spun interface thicknesses determined by SE and NR on the same sample were consistent with each other. Penetration of PVME (T_g = −31 °C) into PS (T_g = 104 °C) was quite rapid at temperatures at least 28 °C below the glass transition of polystyrene and slowed significantly at 35 °C below T_g. SE, with a resolution of ~2 nm, was used to monitor the effect of annealing at 76 °C as the PVME penetration front progressed hundreds of nanometers into the PS phase. It was found that the variation of the penetration depth was markedly non-Fickian, and the observed linear dependence of the depth with time at 76 °C suggests that this is an example of case II diffusion. After annealing at 76 °C, modeling of the SE data with a symmetric interface profile indicated that the interface broadened to ~55 ± 8 nm. Using a symmetric interface profile to model the NR results on the 80 °C annealed samples gave apparent interfaces significantly smaller than 55 nm. This is because the interface is actually asymmetric and NR is mainly sensitive to the maximum gradient in the density profile while SE weights all features of the interface gradient more evenly. By using an asymmetric profile with a low volume fraction PVME extending into the PS phase, a better fit is obtained for both the SE and NR data. This profile is also qualitatively consistent with that determined previously for case II low molecular weight solvent swelling of glassy polymers.

Acknowledgment. We thank G. P. Felcher, A. Karim, R. Goyette, and W. Dozier at Argonne National Laboratory for their input regarding the neutron reflection experiments and for providing the analysis software. We also thank R. J. Composto, E. J. Kramer, M. H. Rafailovich, and J. Sokolov for helpful comments. We thank R. H. Staley for help with the ellipsometry and H. Yu, G. T. Dee, S. R. Lustig, and L. E. Firment for comments on the diffusion of the polymers. The work at the Argonne facility was funded by DOE, BES-Materials Science, under Contract W-31-109-Eng-38.

References and Notes

(1) Werner, S. A.; Klein, A. G. In *Neutron Scattering*; Price, D. L., Skold, K., Eds.; Academic: New York, 1984; Chapter IV.
(2) Arwin, H.; Aspnes, D. E. *Thin Solid Films* **1986**, *138*, 195.
(3) Walsh, D. J.; Sauer, B. B.; Higgins, J. S.; Fernandez, M. L. *Polym. Eng. Sci.* **1990**, *30*, 1085.
(4) Karim, A.; Mansour, A.; Felcher, G. P.; Russell, T. P. Material Research Society Reprints, Fall meeting, 1989.
(5) Fernandez, M. L.; Higgins, J. S.; Penfold, J.; Ward, R. C.; Shackleton, C.; Walsh, D. J. *Polymer* **1988**, *29*, 1923.
(6) Anastasiadis, S. H.; Russell, T. P.; Satija, S. K.; Majkrzak, C. F. *J. Chem. Phys.* **1990**, *92*, 5677.
(7) Stamm, M.; Reiter, G.; Hüttenbach, Foster, M. *ACS Polym. Prepr.* **1990**, *31*, 73.
(8) Sokolov, J.; et al. *ACS Polym. Prepr.* **1990**, *31*, 79.
(9) Russel, T. P.; Karim, A.; Mansour, A.; Felcher, G. P. *Macromolecules* **1988**, *21*, 1890.
(10) Felcher, G. P.; Karim, A.; Russell, T. P. Submitted for publication in *Phys. Rev. B, Rapid Commun.*
(11) Fernandez, M. L.; Higgins, J. S.; Walsh, D. J. *Polymer*, in press.
(12) Rafailovich, M. H.; Sokolov, J.; Jones, R. A. L.; Krausch, G.; Klein, J.; Mills, R. *Europhys. Lett.* **1988**, *5*, 657.
(13) Composto, R. J.; Kramer, E. J. *J. Mater. Sci.* **1991**, *26*, 2815.
(14) Composto, R. J.; Kramer, E. J. Private Communication.
(15) Green, P. F.; Palmstrøm, C. J.; Mayer, J. W.; Kramer, E. J. *Macromolecules* **1985**, *18*, 501.
(16) Turos, A.; Meyer, O. *Nucl. Instrum. Methods* **1984**, *92*, 232.
(17) Green, P. F.; Mills, P. J.; Palmstrøm, C. J.; Mayer, J. W.; Kramer, E. J. *Phys. Rev. Lett.* **1984**, *53*, 2145.
(18) Composto, R. J.; Mayer, J. W.; Kramer, E. J.; White, D. M. *Phys. Rev. Lett.* **1986**, *57*, 1312.
(19) Composto, R. J.; Kramer, E. J.; White, D. M. *Polymer* **1990**, *31*, 2320.
(20) Chaturvedi, U. K.; Steiner, U.; Zak, O.; Krausch, G.; Klein, J. *Phys. Rev. Lett.* **1989**, *63*, 616. Steiner, U.; Krausch, G.; Schatz, G.; Klein, J. *Phys. Rev. Lett.* **1990**, *64*, 1119.
(21) Klein, J. *Science* **1990**, *250*, 640.
(22) Coulon, G.; Russel, T. P.; Deline, V. R.; Green, P. F. *Macromolecules* **1989**, *22*, 2581.
(23) Whitlow, S. J.; Wool, R. P. *Macromolecules* **1989**, *22*, 2648.
(24) Kramer, E. J.; Green, P. F.; Palmstrom, C. J. *Polymer* **1984**, *25*, 473.
(25) Windle, A. H. In *Polymer Permeability*; Comyn, J., Ed.; Elsevier: London, 1985; p. 75.
(26) Mills, P. J.; Kramer, E. J. *J. Mater. Sci.* **1986**, *21*, 4151. Gall, T. P.; Kramer, E. J. *Polymer* **1991**, *32*, 265.
(27) Drude, P. *Ann. Phys.* **1889**, *36*, 532.
(28) Azzam, R. M. A.; Bashara, N. M. In *Ellipsometry and Polarized Light*; North-Holland: New York, 1977.
(29) Born, M.; Wolf, E. In *Principles of Optics*; Pergamon: Oxford, 1975.
(30) Goldberger, M. L.; Seitz, F. *Phys. Rev.* **1947**, *71*, 294.
(31) Cowley, R. A.; Ryan, T. W. *J. Phys. D: Appl. Phys.* **1987**, *20*, 61.
(32) Picot, C. In *Static and Dynamic Properties of the Polymeric Solid State*; Pethrick, R. A., Richards, R. W., Eds.; Reidel: London, 1982; p 127.
(33) Gall, T. P.; Lasky, R. C.; Kramer, E. J. *Polymer* **1990**, *31*, 1491.
(34) Boundy, R. H., Boyer, R. F., Eds. In *Styrene, Its Polymers, Copolymers and Derivatives*; Reinhold Publishing Corp.: New York, 1952.
(35) Lustig, S. R. Ph.D. Thesis, Purdue University, 1989. Lustig, S. R.; Caruthers, J. M.; Peppas, N. A. Submitted for publication in *Chem. Eng. Sci.*
(36) Ben Cheikh Larbi, F.; Leloup, S.; Halary, J. L.; Monnerie, L. *Polym. Commun.* **1986**, *27*, 23.

Registry No. PS, 9003-53-6; PVME, 9003-09-2.